nature communications

Article

https://doi.org/10.1038/s41467-024-54765-2

Sydnthiones are versatile bioorthogonal hydrogen sulfide donors

Received: 9 August 2023

Accepted: 21 November 2024

Published online: 27 November 2024

Check for updates

Wenyuan Xu[1,3], Cheng Tang[1,3], Ruohan Zhao[1,3], Yajun Wang[1,3], Hongyun Jiao[1], Han Ang[1], Yinghan Chen[1] ✉, Xin Wang[2] ✉ & Yong Liang[1,2] ✉

Hydrogen sulfide (H_2S) is an important endogenous gasotransmitter, but the bioorthogonal reaction triggered H_2S donors are still rare. Here we show one type of bioorthogonal H_2S donors, sydnthiones (1,2,3-oxadiazol-3-ium-5-thiolate derivatives), which was designed with the aid of density functional theory (DFT) calculations. The reactions between sydnthiones and strained alkynes provide a platform for controllable, tunable and mitochondria-targeted release of H_2S. We investigate the reactivity of sydnthiones–dibenzoazacyclooctyne (DIBAC) reactions and their orthogonality with two other bioorthogonal cycloaddition pairs: tetrazine–norbornene (Nor) and tetrazine–monohydroxylated cyclooctyne (MOHO). By taking advantage of these mutually orthogonal reactions, we can realize selective labeling or drug release. Furthermore, we explore the role of H_2S, which is released from the sydnthione-DIBAC reaction, on doxorubicin-induced cytotoxicity. The results demonstrate that the viability of H9c2 cells can be significantly improved by pretreating with sydnthione **1b** and DIBAC for 6 h prior to exposure to Dox.

Bioorthogonal reactions have profoundly promoted research in chemical biology and medicinal chemistry over the past two decades[1–3]. Hydrogen sulfide (H_2S), as an endogenous gasotransmitter[4], plays important roles in many physiological processes[5,6]. Carbonyl sulfide (COS), as a precursor of H_2S, can be rapidly hydrolyzed into H_2S in the presence of carbonic anhydrase (CA), which is a ubiquitous enzyme in cells[7]. Although many efforts have been devoted to the development of specific stimuli triggered COS-based H_2S donors[8–20], the example of biocompatible and targeted H_2S release through the bioorthogonal click-and-release reaction is very rare[17,20]. In 2017, Pluth and coworkers used the click-and-release reaction between thiocarbamate-functionalized *trans*-cyclooctene (TCO) and tetrazine to deliver H_2S through the hydrolysis of COS (Fig. 1a)[11]. Although the TCO–tetrazine cycloaddition is super-fast, TCO can easily isomerize in the biological system to generate *cis* isomer that exhibits low reactivity toward tetrazine[3]. Moreover, this H_2S delivery system is invalid in living cells. Due to the high electrophilicity of tetrazine, the released H_2S can be consumed by tetrazine[11]. In 2019, Taran and coworkers first introduced 1,3-dithiolium-4-olate (DTO) into bioorthogonal chemistry[21]. DTO can react with strained alkynes, generating a series of thiophene compounds and releasing an equivalent of COS. Leveraging the click-and-release reaction between 5-(4-carboxyphenyl)-2-(4-diphenylaminophenyl)-1,3-dithiol-1-ium-4-olate (Ph_2N-DTO) and bicyclo-[6.1.0]-nonyne (BCN) (Fig. 1a), our group developed a COS-based H_2S delivery system with a fluorescent thiophene product that allows high spatiotemporal resolution monitoring[17]. Recently, Xian group and Laughlin group successively developed pyranthione-based click-and-release reaction triggered H_2S delivery systems[18,20]. Pyranthiones (PyrS) can react with BCN through a [4+2] cycloaddition, followed by a retro-Diels-Alder reaction to release a molecule of COS (Fig. 1a). In these two H_2S release system, the introduction of a diphenylamino group into DTO (Ph_2N-DTO) and a triphenylphosphorium group into PyrS (PPh_3-PyrS2) can further realize mitochondria-targeted delivery of H_2S in living cells. However, these mitochondria-targeted H_2S donors bearing

[1]State Key Laboratory of Coordination Chemistry, Jiangsu Key Laboratory of Advanced Organic Materials, School of Chemistry and Chemical Engineering, Chemistry and Biomedicine Innovation Center (ChemBIC), ChemBioMed Inter-disciplinary Research Center, Nanjing University, Nanjing 210023, China. [2]Henan-Macquarie University Joint Centre for Biomedical Innovation, School of Life Sciences, Henan University, Kaifeng 475004, China. [3]These authors contributed equally: Wenyuan Xu, Cheng Tang, Ruohan Zhao, Yajun Wang. ✉e-mail: qd_yinghan@163.com; wx@henu.edu.cn; yongliang@nju.edu.cn

https://doi.org/10.1038/s41467-024-54765-2

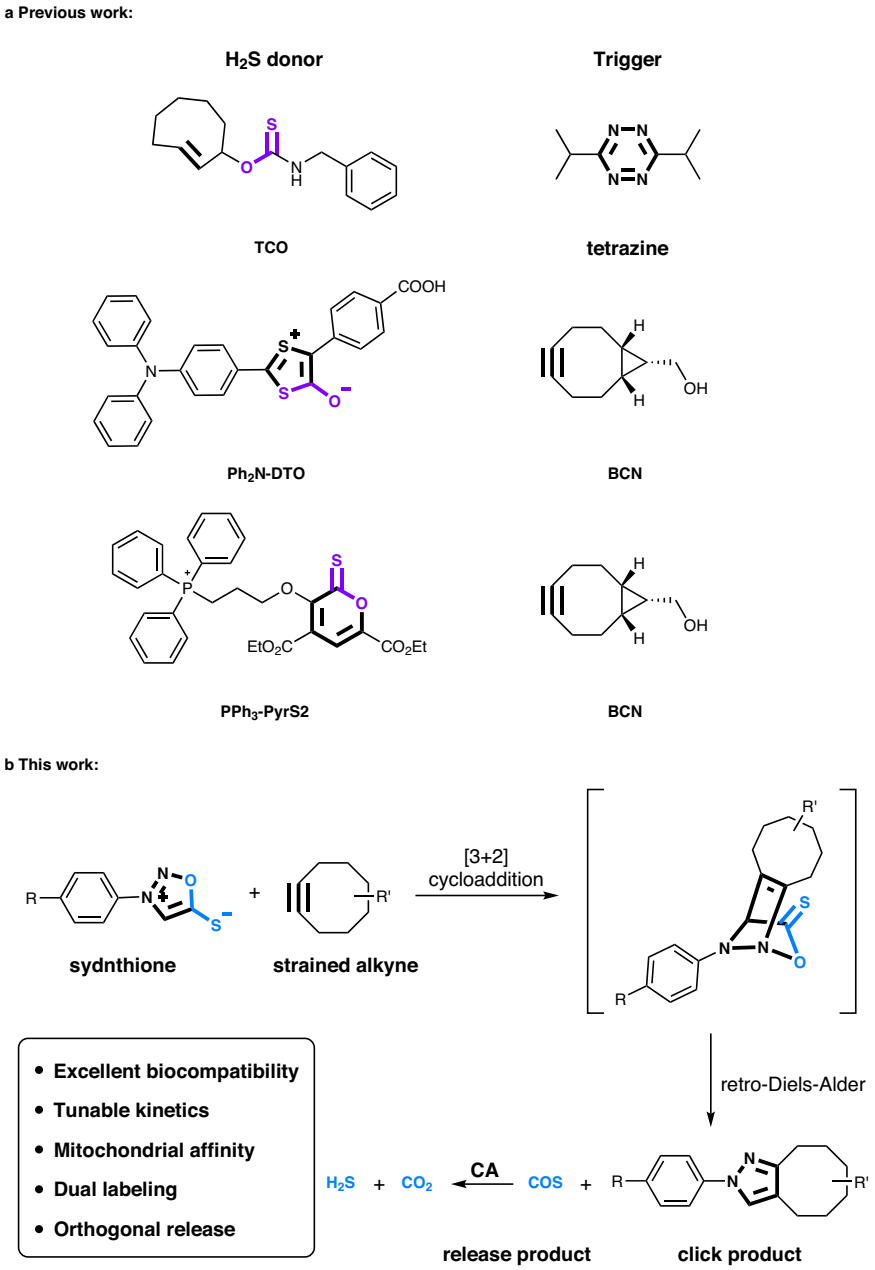

Fig. 1 | Bioorthogonal hydrogen sulfide donors. a Bioorthogonal reaction triggered COS/H_2S donors reported previously[11,17,18,20]. **b** Our design based on the click-and-release reaction between sydnthione and strained alkyne.

three or four phenyl rings lead to the large molecular size and poor water solubility. In addition, the relatively poor stability of Ph_2N-DTO restrained its further biological application, with only 48% of Ph_2N-DTO retained after 24 h of incubation in 3% DMSO/PBS at 37 °C[17]. Mesoionics, a class of five-membered heterocycles, have been employed in organic synthesis and click chemistry[21–37]. Sydnthione (1,2,3-oxadiazol-3-ium-5-thiolate), an exocyclic sulfur substituted sydnone analog, was first reported in 1976[38]. However, to the best of our knowledge, the potential of sydnthiones as bioorthogonal reagents has not been explored.

Studies in complex biological systems require bioorthogonal reactions with mutual orthogonalities. In 2012, Hilderbrand and coworkers discovered mutually orthogonal cycloaddition pairs, tetrazine–TCO and azide–cyclooctyne, and successfully realized simultaneous imaging of two different types of cancer cells[39]. Since then, many groups developed a variety of mutually orthogonal reaction pairs to achieve multiple labeling of biomolecules and cells[26,40–48], and selective delivery of two drugs[29]. Nowadays, with the aid of density functional theory (DFT) calculations, quite a few bioorthogonal reactions and mutually orthogonal cycloaddition pairs have been established[26,29,42–44,49–53].

In this work, we design and synthesize a type of mesoionic compound sydnthiones, which holds great promise in developing biocompatible COS-based H_2S donors. Sydnthiones can undergo bioorthogonal click-and-release reaction with strained alkyne, and the [3+2] cycloaddition would give rise to an equivalent of COS through the subsequent retro-Diels-Alder reaction (Fig. 1b). We use DFT calculations to predict the reactivities of sydnthione with a series of strained alkenes and alkynes, and discover two bioorthogonal click-and-release reactions of sydnthione with BCN and dibenzoazacyclooctyne (DIBAC), which provides a method for H_2S delivery in living cells. More importantly, sydnthione itself shows excellent ability of mitochondrial targeting without any further modification. Furthermore, we identify two

https://doi.org/10.1038/s41467-024-54765-2

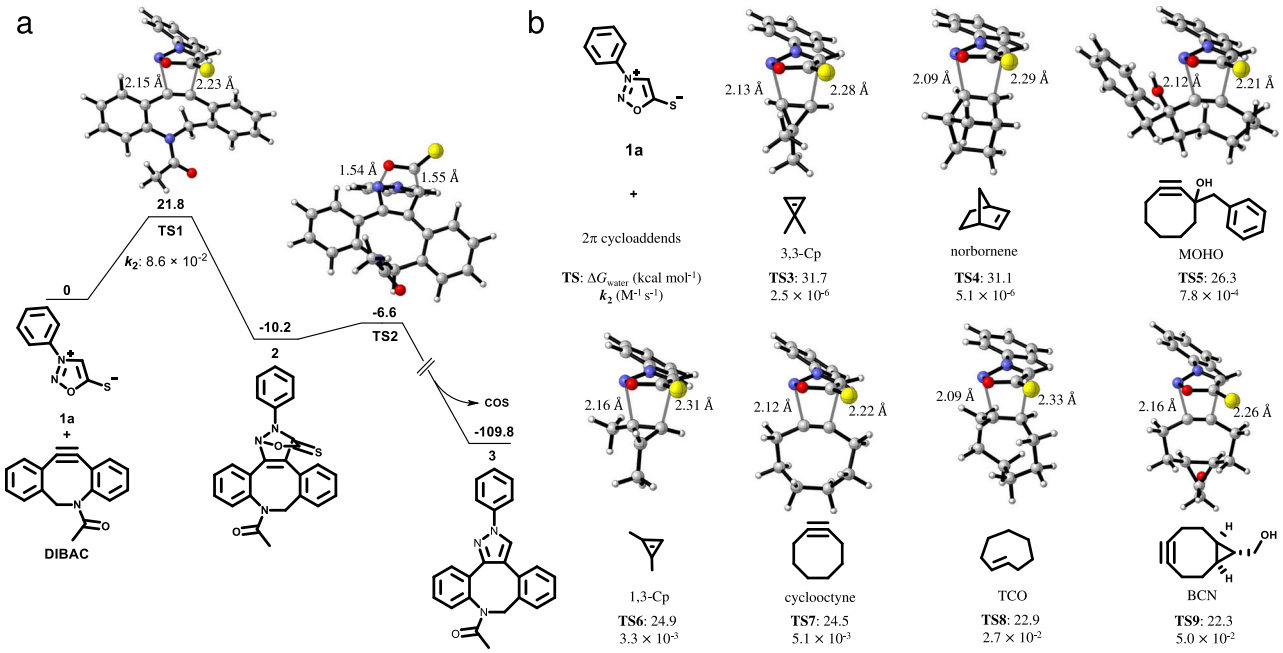

Fig. 2 | DFT calculations on the cycloadditions of *N*-phenyl sydnthione 1a with strained alkenes and alkynes. a DFT-computed Gibbs free energies for the cycloaddition of *N*-phenyl sydnthione **1a** with DIBAC and subsequent COS release. Energies are reported in kcal mol^{-1} and second-order rate constants (k_2) are in M^{-1} s^{-1}. **b** DFT-computed activation free energies for cycloadditions of sydnthione **1a** with strained alkenes and alkynes, and the predicted rate constants in water at 298 K. Calculations were performed at the CPCM(water)-M06-2X/6-311+G(d,p)//M06-2X/6-31G(d) level of theory.

bioorthogonal cycloaddition pairs, tetrazine–norbornene (Nor) and tetrazine–monohydroxylated cyclooctyne (MOHO), which are orthogonal to the sydnthione–DIBAC reaction pair. Exploring the orthogonality of the sydnthione cycloadditions to other bioorthogonal reactions would enable us to study the interactions between H_2S and other molecules in biological systems. Finally, we verify the feasibility of our approach to release H_2S in H9c2 cells and investigated the alleviation effect of H_2S on doxorubicin (Dox)-induced cytotoxicity.

Results

DFT calculations on the cycloadditions of *N*-phenyl sydnthione 1a

In the beginning, we performed DFT calculations on the reaction of *N*-phenyl sydnthione **1a** with DIBAC (Fig. 2a). The [3+2] cycloaddition of **1a** with DIBAC through transition state **TS1** requires an activation free energy of 21.8 kcal mol^{-1}, and the formation of the bridged intermediate **2** is exergonic by 10.2 kcal mol^{-1}. The subsequent retro-Diels-Alder reaction converts **2** into final pyrazole derivative **3** and COS via **TS2** with a barrier of only 3.6 kcal mol^{-1}, which ensures the instantaneous and complete delivery of the desired release product. Therefore, the 1,3-dipolar cycloaddition is predicted to be the rate-determining step of this click-and-release reaction. According to the computed reaction barrier of 21.8 kcal mol^{-1}, the second-order rate constant was predicted to be about 0.1 M^{-1} s^{-1} in water at 298 K after the empirical energy correction, which would be suitable for a bioorthogonal reaction[52]. We further investigated cycloadditions of **1a** with different strained alkenes and alkynes. As shown in Fig. 2b, the predicted rate constants (k_2) range from 10^{-6} to 10^{-2} M^{-1} s^{-1}. Among the eight 2π cycloaddends, DIBAC and BCN are competent partners with sydnthione. However, 3,3-disubstituted cyclopropene (3,3-Cp), Nor, and MOHO are less reactive to sydnthione than DIBAC and BCN based on the predicted rate constants of less than 10^{-3} M^{-1} s^{-1}. In addition, tetrazine, a widely used bioorthogonal reagent, reacts rapidly with Nor[54] and MOHO[55] but not with DIBAC[26,39]. In light of these results, the sydnthione–DIBAC click-and-release reaction should be orthogonal to the known tetrazine–Nor and tetrazine–MOHO cycloadditions.

Synthesis and reactivities of sydnthiones

Inspired by these predictions, we started to synthesize sydnthiones (Fig. 3). First, sydnones **4a-c** were alkylated by the treatment of triethyloxonium tetrafluoroborate. The generated *O*-ethyl sydnones **5a-c** reacted with NaHS in ethanol at −80 °C to give the desired sydnthiones **1a-c** (Fig. 3a). With three different *N*-substituted sydnthiones in hand, we further investigated their reactivities toward DIBAC, BCN, MOHO, and Nor. The kinetics of sydnthiones **1a-c** with DIBAC and BCN are summarized in Table 1. It is found that, for the same sydnthione, DIBAC shows better reactivity (about 3-fold) than BCN. When using the same strained alkyne, sydnthione **1b** with an electron-withdrawing *N*-phenyl group reacts about 6 times faster than sydnthione **1c** with an electron-donating *N*-phenyl group. Overall, the reaction of **1b** with DIBAC has a largest second-order rate constant of 0.113 M^{-1} s^{-1} in 20% DMSO/H_2O at 298 K, while the reaction of **1c** with BCN has a smallest value of 5.2 × 10^{-3} M^{-1} s^{-1}. This means that the release rate of COS can be easily tuned by the electron property of sydnthiones and the employed strained alkynes. Additionally, when sydnthione **1b** was incubated with equimolar amounts of MOHO or Nor in 90% DMSO-d_6/D_2O at 298 K, no reaction was observed even after 24 h (Supplementary Fig. 7). All these experimental results are in good agreement with computational predictions.

Measurement of H_2S release by using the methylene blue assay

In order to confirm the feasibility of the sydnthione as a click-and-release reaction triggered H_2S donor, we measured H_2S release from sydnthione **1b** and DIBAC by using the methylene blue (MB) assay. As shown in bar 1–2 of Fig. 4, **1b** itself cannot spontaneously release H_2S in 20% DMSO/phosphate-buffered saline (PBS, pH 7.4, 10 mM) with or without CA. When sydnthione **1b** (100 μM) was incubated with different equivalents of DIBAC (1–25 eq.) in 20% DMSO/PBS containing CA (25 μg mL^{-1}) at 37 °C, the concentration of released H_2S was enhanced significantly as the equivalents of DIBAC increased (Fig. 4, bar 3–8). Moreover, in the absence of CA or CA being inhibited, much less H_2S was observed (Fig. 4, bar 9–10), indicating the H_2S generation from the hydrolysis of COS.

https://doi.org/10.1038/s41467-024-54765-2

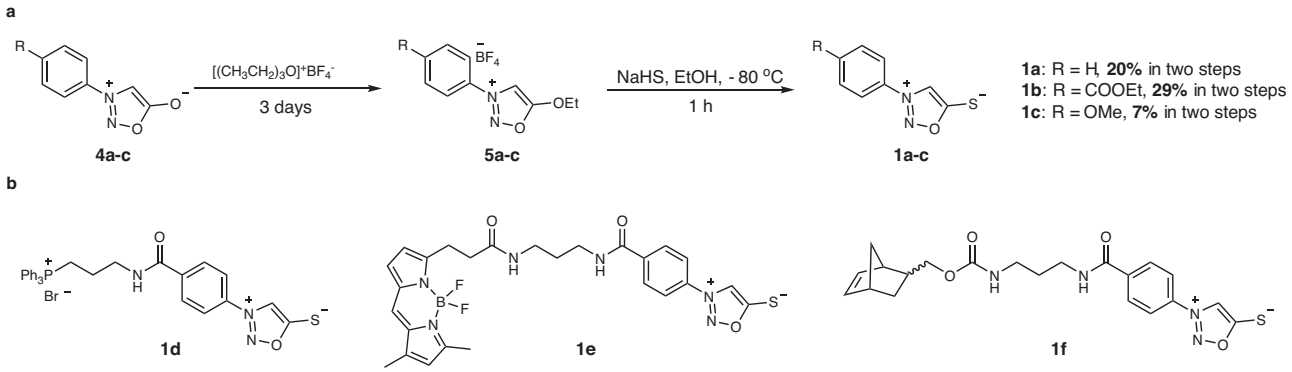

Fig. 3 | The synthesis of sydnthiones. a The synthetic route to sydnthiones **1a-c** from sydnone derivatives **4a-c**. **b** The structures of sydnthione derivatives **1d-f**.

Table 1 | Measured rate constants for reactions between sydnthiones and strained alkynes

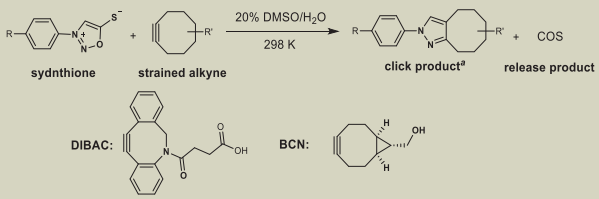

Entry	Sydnthione	Strained alkyne	k_2[b] (M^{-1} s^{-1})[c]
1	1b	DIBAC	0.113 ± 0.003
2	1b	BCN	0.030 ± 0.001
3	1a	DIBAC	0.036 ± 0.016
4	1a	BCN	0.017 ± 0.001
5	1c	DIBAC	0.019 ± 0.002
6	1c	BCN	0.0052 ± 0.0001

[a]Only one regioisomer is depicted.
[b]k_2: second-order rate constants.
[c]Experiments were conducted in triplicate, and results are expressed as mean ± standard derivation (SD) (n = 3 independent samples).

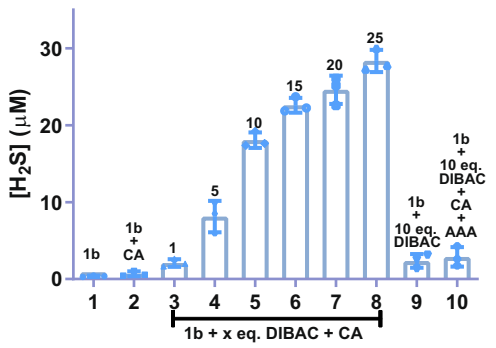

Fig. 4 | H_2S release from the click-and-release reaction between sydnthione 1b and DIBAC. 1b (100 μM) with different reagents in 20% DMSO/PBS (pH 7.4, 10 mM) at 37 °C during 30 min. (1) **1b** only; (2) carbonic anhydrase (CA) (25 μg mL^{-1}); (3) DIBAC (100 μM), CA (25 μg mL^{-1}); (4) DIBAC (500 μM), CA (25 μg mL^{-1}); (5) DIBAC (1.0 mM), CA (25 μg mL^{-1}); (6) DIBAC (1.5 mM), CA (25 μg mL^{-1}); (7) DIBAC (2.0 mM), CA (25 μg mL^{-1}); (8) DIBAC (2.5 mM), CA (25 μg mL^{-1}); (9) DIBAC (1.0 mM); (10) DIBAC (1.0 mM), CA (25 μg mL^{-1}), acetazolamide (AAA) (2.5 μM). Experiments were conducted in triplicate and results are expressed as mean ± SD (n = 3 independent samples). Source data are provided as a Source Data file.

Measurement of H_2S release in living cells

After investigating H_2S release from sydnthione **1b** and DIBAC in vitro, we next demonstrated whether the click-and-release reaction could successfully deliver H_2S in cellular environments. First, we evaluated the stability and toxicity of sydnthione **1b**. After incubating in 10% fetal bovine serum (FBS)/Dulbecco's Modified Eagle Media (DMEM) or H9c2 cell lysate at 37 °C for 24 h, 82% and 89% of sydnthione **1b** remained, respectively (Supplementary Table 1), indicating the excellent stability of **1b**. The incubation of HeLa cells with **1b** did not show cytotoxicity after 24 h even at concentration of 100 μM (Supplementary Fig. 12). Different from in vitro experiments, we used a fluorogenic H_2S probe DCI-CHO-DNP to monitor the liberation of H_2S in cells[56]. DCI-CHO-DNP reacts rapidly with H_2S, inducing the cleavage of diaryl ether to generate 2,4-dinitrobenzenethiol and a fluorescence turn-on product DCI-CHO-OH. HeLa cells were pre-incubated with different concentrations of sydnthione **1b** (0–30 μM) and DCI-CHO-DNP (10 μM) for 30 min, and then treated with 10 equivalents of DIBAC for another 3 h at 37 °C. As depicted in Fig. 5a, when compared with the endogenous H_2S induced red fluorescence, much stronger signals were observed after sydnthione **1b** reacting with DIBAC. An increase in concentrations of sydnthione **1b** resulted in an enhancement of fluorescence intensities, and there is an excellent linear relationship between them (Supplementary Fig. 18, R^2 = 0.994). Furthermore, we measured H_2S release from different substituted sydnthiones **1a-c**. As shown in Fig. 5b, the

https://doi.org/10.1038/s41467-024-54765-2

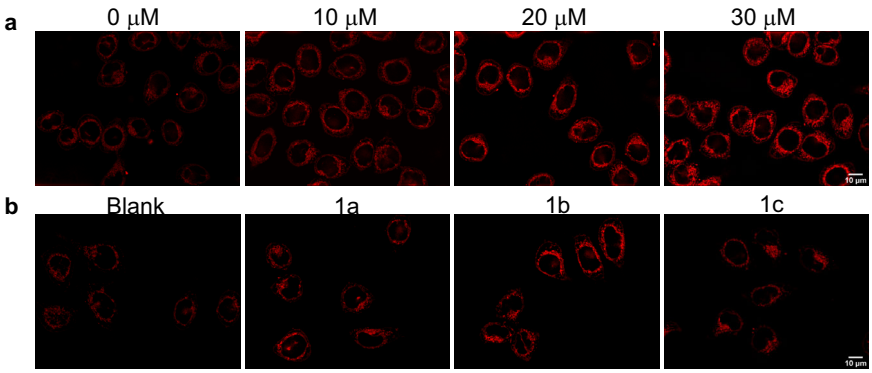

Fig. 5 | Fluorescence images of H_2S release from sydnthione. a Fluorescence images of H_2S release from different concentrations of sydnthione **1b**. HeLa cells were incubated with different concentrations of sydnthione **1b** (0–30 μM) and DCI-CHO-DNP (10 μM) for 30 min, and then treated with 10 eq. of DIBAC for 3 h at 37 °C. **b** Fluorescence images of H_2S release from different sydnthiones. HeLa cells were incubated with sydnthione **1a-c** (30 μM) and DCI-CHO-DNP (10 μM) for 30 min and then treated with 10 eq. of DIBAC for 3 h at 37 °C. Blank: HeLa only treated with 10 μM DCI-CHO-DNP for 3.5 h. Scale bar = 10 μm. The experiment was independently repeated three times with similar results.

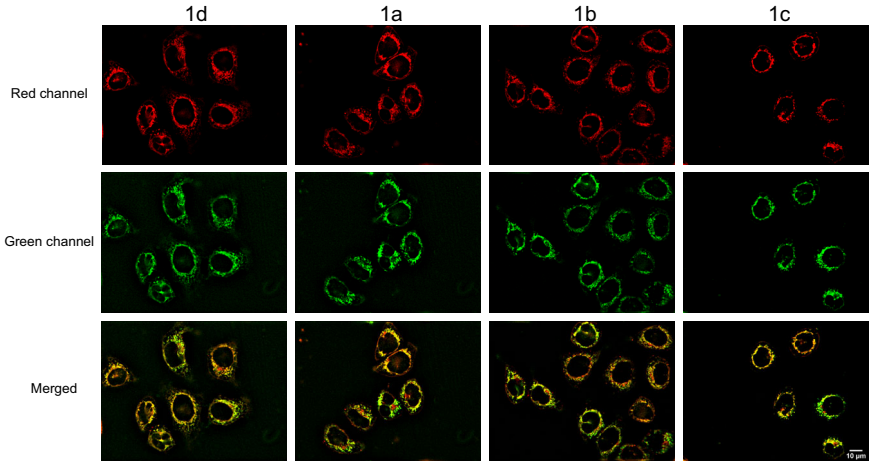

Fig. 6 | Mitochondria-targeted delivery of H_2S in HeLa cells. HeLa cells were pre-incubated with **1a-d** (30 μM) and DCI-CHO-DNP (10 μM) for 30 min, treated with 10 eq. of DIBAC for 3 h at 37 °C, washed, and treated with mito-tracker green (100 nM) for another 30 min. Scale bar = 10 μm. The experiment was independently repeated three times with similar results.

click-and-release reactions between three sydnthiones and DIBAC are all able to deliver exogenous H_2S in HeLa cells. Under the same reaction conditions, sydnthione **1b** showed the strongest red fluorescence, and sydnthione **1c** exhibited the weakest signal. This is consistent with the tendency of measured rate constants shown in Table 1. The relative slow kinetics of sydnthione **1c** and its excellent stability (Supplementary Table 1) makes it a promising slow-releasing H_2S donor for simulating the generation of endogenous H_2S, which has potential applications in H_2S-based therapeutics[57–59].

Mitochondria-targeted H_2S release in living cells

Previous studies have demonstrated that the role of H_2S in cardioprotection is related to mitochondria[60]. However, the reported mitochondria-targeted H_2S donors are rare. AP39, as a known H_2S donor, is targeting to mitochondria by the modification of a triphenylphosphorium group[61]. We introduced a triphenylphosphorium group into the side chain of sydnthione to construct a mitochondria-targeted H_2S donor **1d** (Fig. 3b). As expected, the H_2S release triggered by sydnthione **1d** and DIBAC showed a significant colocalization with the commercial mitochondria-targeting probe mito-tracker green with a Pearson's correlation coefficient of 0.88 (Fig. 6, column 1). To our surprise, the H_2S releases from sydnthiones **1a-c** were also targeting to mitochondria with Pearson's correlation coefficients of 0.79, 0.78, and 0.74, respectively (Fig. 6, column 2–4). To further evaluate the mitochondria-targeting ability of sydnthione, we synthesized a fluorophore-attached sydnthione **1e** (Fig. 3b). Sydnthione **1e** has a distinct mitochondrial distribution with a Pearson's correlation coefficient of 0.79, demonstrating that sydnthione itself is mitochondria-targeting and has minor accumulations in other cellular compartments (Supplementary Fig. 25). Experiments above demonstrated that sydnthiones have great mitochondrial affinity. This feature, combined with the good biocompatibility and small size, will expand the use of sydnthione unit as a structural modification in the mitochondria-targeted research.

Dual labeling in living cells

To apply the mutual orthogonality between sydnthione–DIBAC and tetrazine–Nor cycloaddition pairs in living cells (Fig. 7a), we synthesized norbornene attached sydnthione **1f** (Fig. 3b). When cells were only treated with sydnthione **1f** (Fig. 7b, I), we can only detect faint red fluorescence, as a response to the intrinsic endogenous H_2S. When we incubated HeLa cells with Tz-504 and DIBAC (Fig. 7b, II), only weak background signals could be detected either. These results demonstrate that no reaction occurs either between sydnthione and Nor or

https://doi.org/10.1038/s41467-024-54765-2

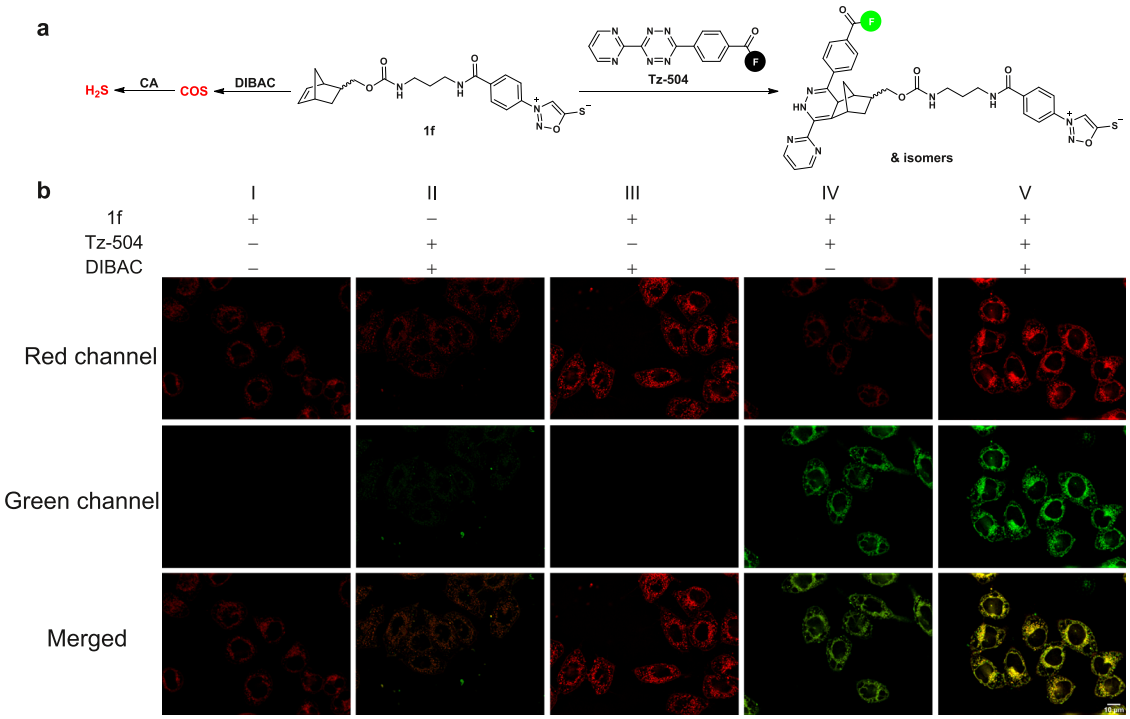

Fig. 7 | Dual labeling in living cells based on mutual orthogonality between sydnthione–DIBAC and tetrazine–Nor bioorthogonal cycloaddition pairs. **a** Mutual orthogonality between sydnthione–DIBAC and tetrazine–Nor bioorthogonal cycloaddition pairs. F: BODIPY. **b** Dual labeling of living cells. I: HeLa cells were incubated with **1f** (30 μM) and DCI-CHO-DNP (10 μM) for 3.5 h at 37 °C. II: HeLa cells were incubated with **Tz-504** (30 μM) and DCI-CHO-DNP (10 μM) for 30 min, and then treated with DIBAC (300 μM) for 3 h at 37 °C. III-V: HeLa cells were incubated with **1f** (30 μM) and DCI-CHO-DNP (10 μM) for 30 min, then treated with either DIBAC (300 μM, III) or **Tz-504** (30 μM, IV) or both (V) for 3 h at 37 °C. Scale bar = 10 μm. The experiment was independently repeated three times with similar results.

between tetrazine and DIBAC. As shown in Fig. 7a, in the reaction of norbornene-attached sydnthione **1f** with DIBAC, only the click-and-release reaction takes place, as evidenced by the distinct red fluorescence in HeLa cells (Fig. 7b, III). Bright green fluorescence can be successfully turned on by the reaction of Tz-504 and **1f** (Fig. 7a, b, IV). The joint incubation with **1f**, DIBAC, and Tz-504 resulted in both red and green fluorescence labeling in HeLa cells (Fig. 7b, V). These experiments indicated the good selectivity of the H_2S release from the sydnthione-DIBAC reaction in the presence of other bioorthogonal reagents, such as tetrazine and norbornene. Furthermore, the inverse-electron-demand Diels-Alder reactions between tetrazine and norbornene have been employed in the delivery of drugs[62,63] and radiopharmaceuticals[64] for cancer therapy. Since these approaches are orthogonal to our H_2S-releasing method, dual-release strategy[65] would provide opportunities to investigate the synergistic effect of H_2S in therapeutic research.

Mutually orthogonal release of H_2S and Dox in living cells

In 2018, Wang and coworkers utilized the click-and-release reaction between Doxorubicin (Dox)-attached tetrazine (**Tz-Dox**) and MOHO to liberate Dox[55]. Our DFT calculations predicted a rate constant of $10^{-4}\,M^{-1}\,s^{-1}$ for the reaction between sydnthione and MOHO (Fig. 2b). This implied a relatively low reactivity, which was later validated by NMR experiments (Supplementary Fig. 7). Therefore, we leveraged the orthogonality between the sydnthione–DIBAC and tetrazine–MOHO reaction pairs toward the selective or simultaneous release of H_2S and Dox in living cells (Fig. 8a). Before the intracellular experiments, we measured the fluorescence property of **Tz-Dox**. As the click-and-release reaction between **Tz-Dox** and MOHO proceeded, fluorescence signals gradually increased (Supplementary Fig. 30), which indicated that the release of Dox can be visualized in living cells. Then we conducted fluorescence imaging experiments to monitor the mutually orthogonal release of H_2S and Dox in H9c2 cells (Fig. 8b). Selective release of H_2S was achieved when H9c2 cells were incubated with **1b, Tz-Dox**, and DIBAC, showing strong red fluorescence of H_2S in the presence of probe DCI-CHO-DNP (Fig. 8b, II). Bright green fluorescence signal of Dox was observed by treating H9c2 cells with **1b, Tz-Dox**, and MOHO (Fig. 8b, III). If we co-treated the cells with **1b, Tz-Dox**, DIBAC, and MOHO, it will result in the concurrent delivery of H_2S (red fluorescence) and Dox (green fluorescence) (Fig. 8b, IV). Taken together, we have identified the first example of mutually orthogonal release of gasotransmitter and drug in living cells.

Sydnthione as H_2S donor in attenuating Dox-induced cardiotoxicity

Dox is a widely used broad-spectrum antineoplastic agent. Its clinical use is often limited by the side effect of cardiotoxicity. Previous studies have demonstrated the potential of H_2S to attenuate Dox-induced toxicity, when co-delivered or released in advance with the administration of Dox[66–70]. Here we conducted experiments to investigate the performance of our H_2S delivery system in alleviating Dox-induced cardiotoxicity. First, we tested the cytotoxicity of the reaction between **1b** and DIBAC on H9c2 cells and showed that it had no obvious effects on cell viability under experimental concentrations (Fig. 9a). Then the effects of simultaneous release of H_2S and Dox were explored. H9c2 cells were treated with different concentrations of sydnthione **1b** (0–12.5 μM) for 30 min before adding 10 equivalents of DIBAC and 10 μM Dox, and then incubated for additional 24 h. As shown in Fig. 9b, 10 μM Dox would lead to around 30–40% cell loss, while co-releasing H_2S was not very efficient to protect cells from Dox toxicity. To our delight, significant improvements in cell viability were observed when H9c2 cells were pretreated with H_2S released from **1b** and DIBAC for 3 h or 6 h prior to exposure to Dox. (Fig. 9c, d). It was found that the toxicity was distinctly attenuated at concentrations as low as 0.8 μM

https://doi.org/10.1038/s41467-024-54765-2

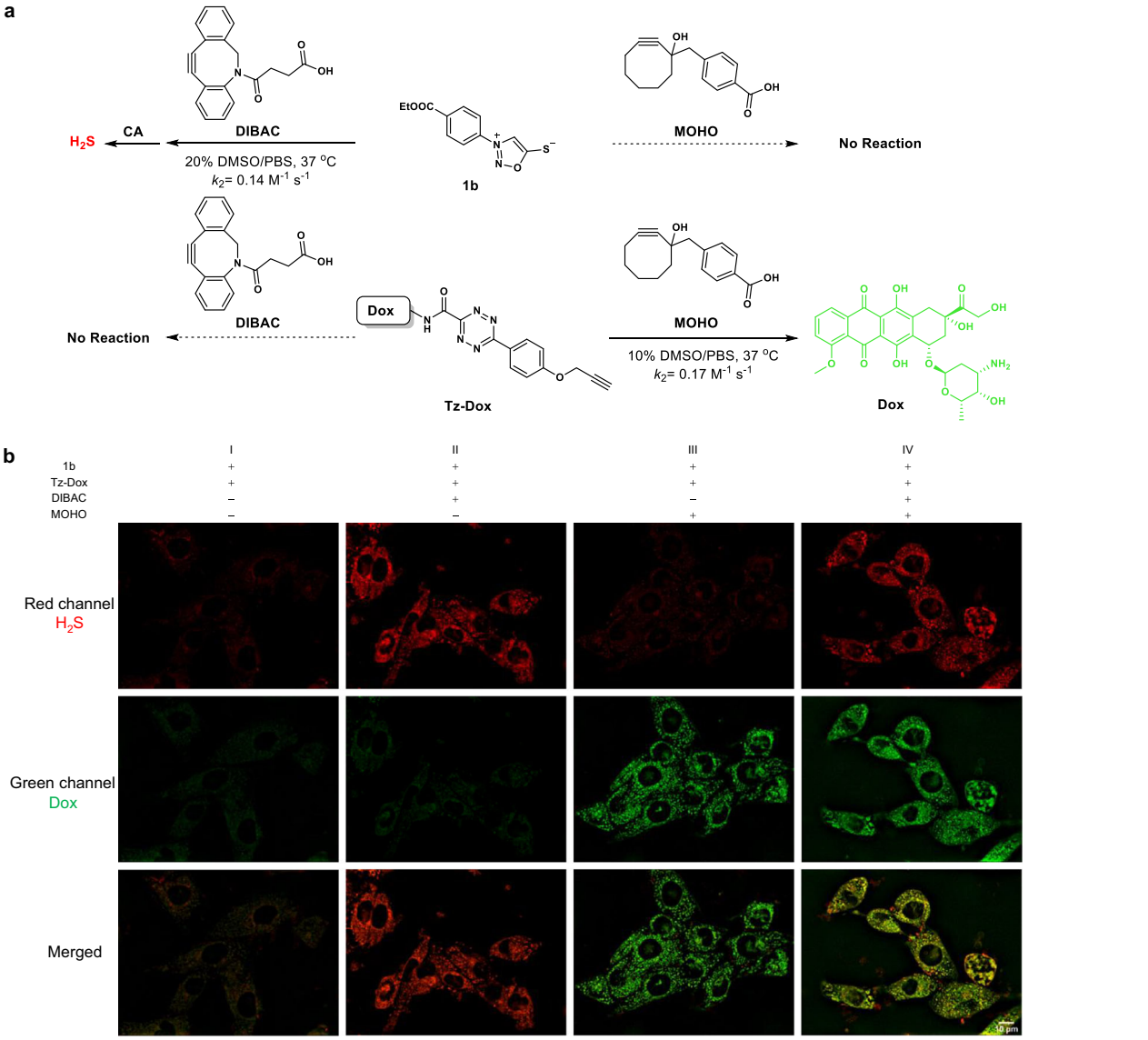

Fig. 8 | Mutually orthogonal release of H_2S and Dox in H9c2 cells based on mutual orthogonality between sydnthione–DIBAC and tetrazine–MOHO bioorthogonal cycloaddition pairs. a Mutual orthogonality between **1b**–DIBAC and **Tz-Dox**–MOHO reaction pairs. **b** Images of orthogonal release of H_2S and Dox in H9c2 cells. I: H9c2 cells were incubated with **1b** (30 μM), **Tz-Dox** (30 μM), and DCI-CHO-DNP (10 μM) for 3.5 h at 37 °C. II-IV: H9c2 cells were incubated with **1b** (30 μM), **Tz-Dox** (30 μM), and DCI-CHO-DNP (10 μM) for 30 min, and then treated with either DIBAC (300 μM, II) or MOHO (300 μM, III) or both (IV) for 3 h at 37 °C. Scale bar = 10 μm. The experiment was independently repeated three times with similar results.

when pretreated H9c2 cells for 6 h, and with 12.5 μM **1b** with DIBAC can almost repair Dox-induced damage. This high efficacy may be due to the mitochondria-targeting H_2S release through our delivery system.

Discussion

In summary, we have developed a type of click-and-release reactions between sydnthiones and strained alkynes, which can be used as a H_2S delivery system with tunable kinetics. We found that sydnthiones exhibit good mitochondria-targeting ability with high stability, low toxicity and small molecular size. Using this H_2S delivery system, we explored the alleviation effects of H_2S on Dox-induced toxicity on H9c2 cells. We found that the toxicity was largely reduced after pretreatment with low concentrations (down to 0.8 μM) of **1b** and DIBAC for 6 h, it may owe to the advantages of mitochondria-targeted H_2S release through our approach. Furthermore, we demonstrated that the sydnthione–DIBAC reaction is orthogonal to both tetrazine–Nor and tetrazine–MOHO cycloadditions, and applied these reactions to selective or simultaneous cell imaging and drug delivery. Overall, we systematically studied the reactivity of sydnthiones and developed a mitochondria-targeting H_2S delivery strategy. We believe that sydnthiones will find diverse applications in chemical biology and hold great promise for therapeutics in the future.

Methods

General information

All chemical reagents were obtained from commercial sources and used without further purification. Thin layer chromatography (TLC) analysis was performed with silica gel-coated plates with 0.2 mm silica gel-coated HSGF 254 plates. Compounds were purified by column chromatography on silica gel (200–300 mesh).

^{1}H NMR and ^{13}C NMR spectra were recorded on a Bruker Avance III 500 MHz or 400 MHz spectrometer. Chemical shifts for ^{1}H NMR spectra are reported as δ in units of parts per million (ppm) downfield from $SiMe_4$ (δ 0.0) and relative to the signal of chloroform-*d* ($CDCl_3$) (δ 7.26, singlet). Multiplicities were given as: s (singlet); d (doublet); t (triplet); q (quartet); dd (doublets of doublet) or m (multiplets). The

https://doi.org/10.1038/s41467-024-54765-2

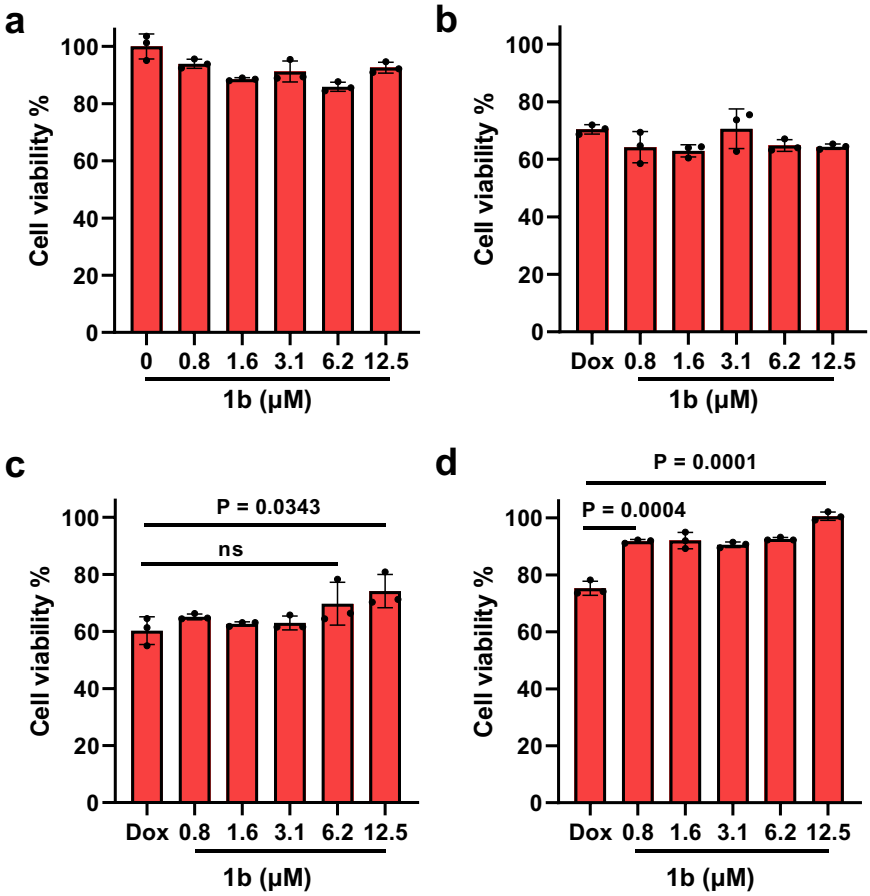

Fig. 9 | Effects on cell viability through the release of H_2S from sydnthione 1b in Dox-treated H9c2 cells. a H9c2 cells were treated with **1b** (0–12.5 μM) at 37 °C for 30 min, then incubated with 10 eq. DIBAC for 6 h. Cells were then treated with DMSO for additional 24 h. **b** H9c2 cells were treated with **1b** (0–12.5 μM) at 37 °C for 30 min, then incubated with 10 eq. DIBAC and 10 μM Dox for 24 h. **c**, **d** H9c2 cells were treated with **1b** (0–12.5 μM) at 37 °C for 30 min, then incubated with 10 eq. DIBAC for **c** 3 h or **d** 6 h. Cells were then treated with 10 μM Dox for additional 24 h. Data are presented as mean ± SD ($n = 3$ independent cell pellets). Statistical differences were analyzed by Student's two-sided *t*-test between Ctrl and indicated groups. ns, not significant. Source data are provided as a Source Data file.

number of protons (n) for a given resonance is indicated by nH. Coupling constants are reported as a *J* value in Hertz. Chemical shifts for ^{13}C NMR spectra are reported as δ in units of ppm downfield from $SiMe_4$ (δ 0.0) and relative to the signal of $CDCl_3$ (δ 77.16, triplet). High-resolution mass spectra (HRMS) analyses were performed on an Agilent quadrupole time flight high-resolution mass spectrometer mass spectrometer (6540 Q-TOF LC/MS). Liquid chromatogram was detected by Shimadzu HPLC (LC-20AD, SPD-M20A detector). Analyses were performed using an ACE Excel 5 C18-Amide column (250 × 4.6 mm, id) at a flow rate of 1 mL min^{-1}. 3-(4,5-Dimethylthiazol-2-yl)-2,5-diphenyltertrazolium bromide (MTT) assay was performed on a microplate reader (Tcan). Fluorescence spectra were recorded at room temperature by LS55 (PE, America) spectrophotometer from molecular devices using a cuvette with 1 cm path length. Fluorescence microscopy images were taken on an Olympus IX73 fluorescent inverted microscope. Flow cytometry was conducted with Agilent NovoCyte, and data were analyzed and processed using FlowJo.

Computational details

All calculations were performed with Gaussian 09[71]. Geometry optimizations of all the minima and transition structures were carried out at the M06-2X level of theory[72–74] with the 6-31 G(d) basis set. Vibrational frequencies were evaluated at the same level to verify that optimized structure is an energy minimum or a transition state and to compute zero-point vibrational energies (ZPVE) and thermal corrections at 298 K. Solvent effects in water were calculated at the M06-2X/6-311+G(d,p) level using the gas-phase optimized structures with the CPCM model[75–77], where UFF radii were used. The predicted second-order rate constants shown in Fig. 2 were calculated by using the corrected activation free energies [$\Delta G^{\ddagger}_{corr} = (\Delta G^{\ddagger}_{compt} + 8.4)/1.6$][52], according to Eyring equation at 298 K.

Kinetics measurement

The kinetics of cycloadditions of sydnthione **1** with DIBAC or BCN were measured by HPLC in 20% DMSO/H_2O at room temperature. Stock solutions of sydnthione **1**, DIBAC, BCN and internal standard in DMSO were prepared. Prepared respective concentration solutions in 20% DMSO/H_2O, leading to the final concentration of sydnthione **1** and internal standard were 25 μM, DIBAC and BCN were 250 μM. Reactions were monitored by the absorption peak area of sydnthione **1** as compared with the internal standard. Consumption of materials followed a second-order equation (Eq. (1)) and the second-order rate constants were obtained by least squares fitting of the data to a linear equation. Experiments were conducted in triplicate, and results are expressed as mean ± standard derivation (SD) ($n = 3$).

$$-\ln[A] = k_2[B]_0 t + \text{const} \quad (1)$$

[A]: concentration of sydnthione **1** (M)
$[B]_0$: initial concentration of DIBAC (M)
k_2: second-order rate constant (M^{-1} s^{-1})

The kinetics of cycloaddition of sydnthione **1b** with DIBAC at 37 °C was measured by HPLC in 20% DMSO/PBS (pH 7.4, 10 mM). Stock solutions of sydnthione **1b** and DIBAC in DMSO were prepared. Prepared respective concentration solutions in 20% DMSO/PBS (pH 7.4, 10 mM), leading to the final concentration of sydnthione **1b** was 100 μM and DIBAC was 1 mM. Reactions were monitored by the absorption peak area of sydnthione **1b**. Consumption of materials followed a second-order equation (Eq. (1)) and the second-order rate constants were obtained by least squares fitting of the data to a linear equation. Experiments were conducted in triplicate, and results are expressed as mean ± standard derivation (SD) ($n = 3$ independent samples).

Detection of H_2S release in living cells

Cells were seeded in 4-Chamber Glass Bottom Dish and incubated overnight at 37 °C with 5% CO_2. Test compound was dissolved in DMSO to prepare a stock solution. After attachment, HeLa cells were pre-incubated with sydnthione and DCI-CHO-DNP for 30 min, then treated with DIBAC at 37 °C. Then the cells were washed and the microscopy images were taken on using the red channel (excitation: 540–580 nm, emission: 590 nm to near-infrared) with 60× magnification on an Olympus IX73 fluorescent inverted microscope.

Mitochondria-targeted delivery of H_2S in HeLa cells

Cells were seeded in 4-Chamber Glass Bottom Dish and incubated overnight at 37 °C with 5% CO_2. Test compound was dissolved in DMSO to prepare a stock solution. After attachment, HeLa cells were pre-incubated with 30 μM sydnthione and 10 μM DCI-CHO-DNP for 30 min, then treated with 10 eq. of DIBAC for 3 h at 37 °C, washed and treated with 100 nM mito-tracker green for another 30 min. Then the cells were washed, and the microscopy images were taken using the green channel (excitation: 470–495 nm, emission: 510–550 nm) and the red channel (excitation: 540–580 nm, emission: 590 nm to near-infrared) with 60× magnification on an Olympus IX73 fluorescent inverted microscope.

Sydnthione in attenuating Dox-induced cardiotoxicity

H9c2 cells (1×10^4/well) were seeded into 96-well plates and cultured for 24 h. For H_2S and Dox were delivered simultaneously, the cells were treated with **1b** (0–12.5 μM) at 37 °C for 30 min, then incubated with 10 eq. DIBAC and 10 μM Dox for 24 h. For H_2S was delivered first, the cells were treated with **1b** (0–12.5 μM) at 37 °C for 30 min, then incubated with 10 eq. DIBAC for 3 h or 6 h. Cells were then treated with 10 μM Dox or DMSO for an additional 24 h. Cell viability was tested by MTT kit (Keygen Biotech Co., Ltd., Nanjing, China). 50 μL 1 x MTT was added to each well. After incubating at 37 °C in 5% CO_2 for another 4 h, the medium was replaced with 150 μL DMSO. Then, absorbance at 490 nm was measured.

Reporting summary

Further information on research design is available in the Nature Portfolio Reporting Summary linked to this article.

Data availability

The experimental data supporting the findings of this study are available within the article and Supplementary Information, and from the corresponding author(s) upon request. The data for all graphs generated in this study are provided in the Source Data files. The source data for fluorescence images are available in Figshare https://figshare.com/s/6cc272aa2d58e90ed26d. The Supplementary Calculation Data for this article is available as a separate Supplementary Data file. The HPLC profiles for the stability studies are available as a separate Supplementary Data file. Source data are provided with this paper.

References

1. Devaraj, N. K. The future of bioorthogonal chemistry. *ACS Cent. Sci.* **4**, 952–959 (2018).
2. Nguyen, S. S. & Prescher, J. A. Developing bioorthogonal probes to span a spectrum of reactivities. *Nat. Rev. Chem.* **4**, 476–489 (2020).
3. Rigolot, V., Biot, C. & Lion, C. To view your biomolecule, click inside the cell. *Angew. Chem. Int. Ed.* **60**, 23084–23105 (2021).
4. Wang, R. Two's company, three's a crowd: can H_2S be the third endogenous gaseous transmitter? *FASEB J.* **16**, 1792–1798 (2002).
5. Wallace, J. L. & Wang, R. Hydrogen sulfide-based therapeutics: exploiting a unique but ubiquitous gasotransmitter. *Nat. Rev. Drug Discov.* **14**, 329–345 (2015).
6. Hartle, M. D. & Pluth, M. D. A practical guide to working with H_2S at the interface of chemistry and biology. *Chem. Soc. Rev.* **45**, 6108–6117 (2016).
7. Mishra, C. B., Tiwari, M. & Supuran, C. T. Progress in the development of human carbonic anhydrase inhibitors and their pharmacological applications: where are we today? *Med. Res. Rev.* **40**, 2485–2565 (2020).
8. Levinn, C. M., Cerda, M. M. & Pluth, M. D. Development and application of carbonyl sulfide-based donors for H_2S delivery. *Acc. Chem. Res.* **52**, 2723–2731 (2019).
9. Steiger, A. K., Pardue, S., Kevil, C. G. & Pluth, M. D. Self-immolative thiocarbamates provide access to triggered H_2S donors and analyte replacement fluorescent probes. *J. Am. Chem. Soc.* **138**, 7256–7259 (2016).
10. Zhao, Y. & Pluth, M. D. Hydrogen sulfide donors activated by reactive oxygen species. *Angew. Chem. Int. Ed.* **55**, 14638–14642 (2016).
11. Steiger, A. K., Yang, Y., Royzen, M. & Pluth, M. D. Bio-orthogonal "click-and-release" donation of caged carbonyl sulfide (COS) and hydrogen sulfide (H_2S). *Chem. Commun.* **53**, 1378–1380 (2017).
12. Zhao, Y., Henthorn, H. A. & Pluth, M. D. Kinetic insights into hydrogen sulfide delivery from caged-carbonyl sulfide isomeric donor platforms. *J. Am. Chem. Soc.* **139**, 16365–16376 (2017).
13. Zhao, Y., Steiger, A. K. & Pluth, M. D. Colorimetric carbonyl sulfide (COS)/hydrogen sulfide (H_2S) donation from γ-ketothiocarbamate donor motifs. *Angew. Chem. Int. Ed.* **57**, 13101–13105 (2018).
14. Zhao, Y., Henthorn, H. A. & Pluth, M. D. Cyclic sulfenyl thiocarbamates release carbonyl sulfide and hydrogen sulfide independently in thiol-promoted pathways. *J. Am. Chem. Soc.* **141**, 13610–13618 (2019).
15. Hu, Y. et al. Reactive oxygen species-triggered off-on fluorescence donor for imaging hydrogen sulfide delivery in living cells. *Chem. Sci.* **10**, 7690–7694 (2019).
16. Zhao, Y., Cerda, M. M. & Pluth, M. D. Fluorogenic hydrogen sulfide (H_2S) donors based on sulfenyl thiocarbonates enable H_2S tracking and quantification. *Chem. Sci.* **10**, 1873–1878 (2019).
17. Chen, Y. et al. Design and development of a bioorthogonal, visualizable and mitochondria-targeted hydrogen sulfide (H_2S) delivery system. *Angew. Chem. Int. Ed.* **61**, e202112734 (2022).
18. Cui, Q. et al. Controllable cycloadditions between 2*H*-(Thio)pyran-2-(thi)ones and strained alkynes: a click-and-release strategy for COS/H_2S generation. *Org. Lett.* **24**, 7334–7338 (2022).
19. Gilbert, A. K. & Pluth, M. D. Subcellular delivery of hydrogen sulfide using small molecule donors impacts organelle stress. *J. Am. Chem. Soc.* **144**, 17651–17660 (2022).
20. Huang, W., Gunawardhana, N., Zhang, Y., Escorihuela, J. & Laughlin, S. T. Pyranthiones/pyrones: "click and release" donors for subcellular hydrogen sulfide delivery and labeling. *Chem. Eur. J.* **30**, e202303465 (2024).
21. Kumar, R. A. et al. Strain-promoted 1,3-dithiolium-4-olates-alkyne cycloaddition. *Angew. Chem. Int. Ed.* **58**, 14544–14548 (2019).
22. Browne, D. L. & Harrity, J. P. A. Recent developments in the chemistry of sydnones. *Tetrahedron* **66**, 553–568 (2010).
23. Decuypère, E., Plougastel, L., Audisio, D. & Taran, F. Sydnone-alkyne cycloaddition: applications in synthesis and bioconjugation. *Chem. Commun.* **53**, 11515–11527 (2017).

24. Porte, K., Riomet, M., Figliola, C., Audisio, D. & Taran, F. Click and bio-orthogonal reactions with mesoionic compounds. *Chem. Rev.* **121**, 6718–6743 (2021).
25. Wallace, S. & Chin, J. W. Strain-promoted sydnone bicyclo-[6.1.0]-nonyne cycloaddition. *Chem. Sci.* **5**, 1742–1744 (2014).
26. Narayanam, M. K., Liang, Y., Houk, K. N. & Murphy, J. M. Discovery of new mutually orthogonal bioorthogonal cycloaddition pairs through computational screening. *Chem. Sci.* **7**, 1257–1261 (2016).
27. Narayanam, M. K., Ma, G., Champagne, P. A., Houk, K. N. & Murphy, J. M. Synthesis of [^{18}F] fluoroarenes by nucleophilic radiofluorination of *N*-arylsydnones. *Angew. Chem. Int. Ed.* **56**, 13006–13010 (2017).
28. Bernard, S. et al. Bioorthogonal click and release reaction of iminosydnones with cycloalkynes. *Angew. Chem. Int. Ed.* **56**, 15612–15616 (2017).
29. Shao, Z. et al. Bioorthogonal release of sulfonamides and mutually orthogonal liberation of two drugs. *Chem. Commun.* **54**, 14089–14092 (2018).
30. Shao, Z. et al. Design of a 1,8-naphthalimide-based OFF-ON type bioorthogonal reagent for fluorescent imaging in live cells. *Chin. Chem. Lett.* **30**, 2169–2172 (2019).
31. Richard, M. et al. New fluorine-18 pretargeting PET imaging by bioorthogonal chlorosydnone-cycloalkyne click reaction. *Chem. Commun.* **55**, 10400–10403 (2019).
32. Porte, K. et al. Controlled release of a micelle payload via sequential enzymatic and bioorthogonal reactions in living systems. *Angew. Chem. Int. Ed.* **58**, 6366–6370 (2019).
33. Dovgan, I. et al. Automated linkage of proteins and payloads producing monodisperse conjugates. *Chem. Sci.* **11**, 1210–1215 (2020).
34. Narayanam, M. K. et al. Positron emission tomography tracer design of targeted synthetic peptides via ^{18}F-sydnone alkyne cycloaddition. *Bioconjug. Chem.* **32**, 2073–2082 (2021).
35. Xu, W. et al. Fluorogenic sydnonimine probes for orthogonal labeling. *Org. Biomol. Chem.* **20**, 5953–5957 (2022).
36. Ribéraud, M. et al. Fast and bioorthogonal release of isocyanates in living cells from iminosydnones and cycloalkynes. *J. Am. Chem. Soc.* **145**, 2219–2229 (2023).
37. Zhao, R., Chen, Y. & Liang, Y. Bioorthogonal delivery of carbon disulfide in living cells. *Angew. Chem. Int. Ed.* **63**, e202400020 (2024).
38. Hanley, R. N., Ollis, W. D. & Ramsden, C. A. Synthesis of 3 new mesoionic heterocyclic-systems. *J. Chem. Soc. Chem. Commun* **1976**, 306–307 (1976).
39. Karver, M. R., Weissleder, R. & Hilderbrand, S. A. Bioorthogonal reaction pairs enable simultaneous, selective, multi-target imaging. *Angew. Chem. Int. Ed.* **51**, 920–922 (2012).
40. Patterson, D. M., Nazarova, L. A., Xie, B., Kamber, D. N. & Prescher, J. A. Functionalized cyclopropenes as bioorthogonal chemical reporters. *J. Am. Chem. Soc.* **134**, 18638–18643 (2012).
41. Sachdeva, A., Wang, K. H., Elliott, T. & Chin, J. W. Concerted, rapid, quantitative, and site-specific dual labeling of proteins. *J. Am. Chem. Soc.* **136**, 7785–7788 (2014).
42. Tu, J. et al. Stable, reactive, and orthogonal tetrazines: dispersion forces promote the cycloaddition with isonitriles. *Angew. Chem. Int. Ed.* **58**, 9043–9048 (2019).
43. Kamber, D. N. et al. Isomeric triazines exhibit unique profiles of bioorthogonal reactivity. *Chem. Sci.* **10**, 9109–9114 (2019).
44. Hu, Y. et al. Triple, mutually orthogonal bioorthogonal pairs through the design of electronically activated sulfamate-containing cycloalkynes. *J. Am. Chem. Soc.* **142**, 18826–18835 (2020).
45. Xi, Z. et al. Metal- and strain-free bioorthogonal cycloaddition of *o*-diones with furan-2(3*H*)-one as anionic cycloaddend. *Angew. Chem. Int. Ed.* **61**, e202200239 (2022).
46. Zhang, X. et al. Isonitrile induced bioorthogonal activation of fluorophores and mutually orthogonal cleavage in live cells. *Chem. Commun.* **58**, 573–576 (2022).
47. Peschke, F., Taladriz-Sender, A., Andrews, M. J., Watson, A. J. B. & Burley, G. A. Glutathione mediates control of dual differential bioorthogonal labelling of biomolecules. *Angew. Chem. Int. Ed.* **62**, e202313063 (2023).
48. Wang, Y. et al. Noncanonical amino acids as doubly bio-orthogonal handles for one-pot preparation of protein multiconjugates. *Nat. Commun.* **14**, 974 (2023).
49. Liang, Y., Mackey, J. L., Lopez, S. A., Liu, F. & Houk, K. N. Control and design of mutual orthogonality in bioorthogonal cycloadditions. *J. Am. Chem. Soc.* **134**, 17904–17907 (2012).
50. Kamber, D. N. et al. Isomeric cyclopropenes exhibit unique bioorthogonal reactivities. *J. Am. Chem. Soc.* **135**, 13680–13683 (2013).
51. Yang, J., Liang, Y., Šečkutė, J., Houk, K. N. & Devaraj, N. K. Synthesis and reactivity comparisons of 1-methyl-3-substituted cyclopropene mini-tags for tetrazine bioorthogonal reactions. *Chem. Eur. J.* **20**, 3365–3375 (2014).
52. Liu, F., Liang, Y. & Houk, K. N. Bioorthogonal cycloadditions: computational analysis with the distortion/interaction model and predictions of reactivities. *Acc. Chem. Res.* **50**, 2297–2308 (2017).
53. Kang, D. & Kim, J. Bioorthogonal retro-cope elimination reaction of *N,N*-dialkylhydroxylamines and strained alkynes. *J. Am. Chem. Soc.* **143**, 5616–5621 (2021).
54. Devaraj, N. K., Weissleder, R. & Hilderbrand, S. A. Tetrazine-based cycloadditions: application to pretargeted live cell imaging. *Bioconjug. Chem.* **19**, 2297–2299 (2008).
55. Zheng, Y. et al. Enrichment-triggered prodrug activation demonstrated through mitochondria-targeted delivery of doxorubicin and carbon monoxide. *Nat. Chem.* **10**, 787–794 (2018).
56. Hong, J., Zhou, E., Gong, S. & Feng, G. A red to near-infrared fluorescent probe featuring a super large Stokes shift for light-up detection of endogenous H_2S. *Dyes Pigments* **160**, 787–793 (2019).
57. Andreadou, I. et al. The role of gasotransmitters NO, H_2S, CO in myocardial ischemia/reperfusion injury and cardioprotection by preconditioning, postconditioning, and remote conditioning. *Br. J. Pharmacol.* **172**, 1587–1606 (2015).
58. Zheng, Y. et al. Toward hydrogen sulfide based therapeutics: critical drug delivery and developability issues. *Med. Res. Rev.* **38**, 57–100 (2018).
59. Levinn, C. M., Cerda, M. M. & Pluth, M. D. Activatable small-molecule hydrogen sulfide donors. *Antioxid. Redox Signal.* **32**, 96–109 (2020).
60. Calvert, J. W., Coetzee, W. A. & Lefer, D. J. Novel insights into hydrogen sulfide-mediated cytoprotection. *Antioxid. Redox Signal.* **12**, 1203–1217 (2010).
61. Szczesny, B. et al. AP39, a novel mitochondria-targeted hydrogen sulfide donor, stimulates cellular bioenergetics, exerts cytoprotective effects and protects against the loss of mitochondrial DNA integrity in oxidatively stressed endothelial cells in vitro. *Nitric Oxide* **41**, 120–130 (2014).
62. Kannaka, K. et al. Synthesis of an amphiphilic tetrazine derivative and its application as a liposomal component to accelerate release of encapsulated drugs. *Bioorg. Med. Chem.* **27**, 3613–3618 (2019).
63. Kannaka, K. et al. Inverse electron demand Diels-Alder reactions in the liposomal membrane accelerates release of the encapsulated drugs. *Langmuir* **36**, 10750–10755 (2020).
64. Zeglis, B. et al. Modular strategy for the construction of radiometalated antibodies for positron emission tomography based on inverse electron demand Diels-Alder click chemistry. *Bioconjug. Chem.* **22**, 2048–2059 (2011).
65. Tu, J. et al. Isonitrile-responsive and bioorthogonally removable tetrazine protecting groups. *Chem. Sci.* **11**, 169–179 (2020).
66. Wang, X.-Y. et al. Hydrogen sulfide protects H9c2 cells against doxorubicin-induced cardiotoxicity through inhibition of endoplasmic reticulum stress. *Mol. Cell. Biochem.* **363**, 419–426 (2012).

67. Guo, R. et al. Exogenous hydrogen sulfide protects against doxorubicin-induced inflammation and cytotoxicity by inhibiting p38MAPK/NFκB pathway in H9c2 cardiac cells. *Cell. Physiol. Biochem.* **32**, 1668–1680 (2013).
68. Liu, M. H. et al. Hydrogen sulfide attenuates doxorubicin-induced cardiotoxicity by inhibiting calreticulin expression in H9c2 cells. *Mol. Med. Rep.* **12**, 5197–5202 (2015).
69. Chegaev, K. et al. H_2S-donating doxorubicins may overcome cardiotoxicity and multidrug resistance. *J. Med. Chem.* **59**, 4881–4889 (2016).
70. Hu, Q. et al. Mitigation of doxorubicin-induced cardiotoxicity with an H_2O_2-activated, H_2S-donating hybrid prodrug. *Redox Biol.* **53**, 102338 (2022).
71. Frisch, M. J. et al. Gaussian 09, revision D.01 (Gaussian Inc., 2013).
72. Zhao, Y. & Truhlar, D. G. The M06 suite of density functionals for main group thermochemistry, thermochemical kinetics, noncovalent interactions, excited states, and transition elements: two new functionals and systematic testing of four M06-class functionals and 12 other functionals. *Theor. Chem. Acc.* **120**, 215–241 (2008).
73. Zhao, Y. & Truhlar, D. G. Density functionals with broad applicability in chemistry. *Acc. Chem. Res.* **41**, 157–167 (2008).
74. Zhao, Y. & Truhlar, D. G. Computational characterization and modeling of buckyball tweezers: density functional study of concave–convex π-π interactions. *Phys. Chem. Chem. Phys.* **10**, 2813–2818 (2008).
75. Barone, V. & Cossi, M. Quantum calculation of molecular energies and energy gradients in solution by a conductor solvent model. *J. Phys. Chem. A* **102**, 1995–2001 (1998).
76. Cossi, M., Rega, N., Scalmani, G. & Barone, V. Energies, structures, and electronic properties of molecules in solution with the C-PCM solvation model. *J. Comput. Chem.* **24**, 669–681 (2003).
77. Takano, Y. & Houk, K. N. Benchmarking the conductor-like polarizable continuum model (CPCM) for aqueous solvation free energies of neutral and ionic organic molecules. *J. Chem. Theory Comput.* **1**, 70–77 (2005).

Acknowledgements

We thank the National Key R&D Program of China (2022YFA1503200, Y.L.), the National Natural Science Foundation of China (22207051, Y.C., 22303027, W.X., and 22077062, Y.L.), and the Natural Science Foundation of Jiangsu Province (BK20220766, Y.C., and BK20230018, Y.L.) for financial supports. We thank the High Performance Computing Center (HPCC) of Nanjing University for doing the numerical calculations in this paper on its blade cluster system.

Author contributions

Y.L., W.X. and Y.C. conceived and supervised the project. W.X. and Y.L. designed the experiments and wrote the paper. W.X., C.T., R.Z., Y.W., H.J., H.A. and Y.C. performed the experiments. W.X. and X.W. performed the DFT calculations.

Competing interests

The authors declare no competing interests.

Additional information

Supplementary information The online version contains supplementary material available at https://doi.org/10.1038/s41467-024-54765-2.

Correspondence and requests for materials should be addressed to Yinghan Chen, Xin Wang or Yong Liang.

Peer review information *Nature Communications* thanks Yanira Mendez-Gomez and the other anonymous reviewer(s) for their contribution to the peer review of this work. A peer review file is available.